

# A Study of Shelterbelt Transpiration and Cropland Evapotranspiration in an Irrigated Area in the Middle Reaches of the Heihe River in Northwestern China

Chen Qiao, Rui Sun, Ziwei Xu, Lei Zhang, Liangyun Liu, Lvyuan Hao, and Guoqing Jiang

**Abstract**—The transpiration from shelterbelts and the evapotranspiration (ET) from cropland (maize and vegetables) and orchards (apple) in an irrigated area in the middle reaches of the Heihe River, China, were estimated using a modified Penman–Monteith (P-M) formula and airborne remote sensing data. The results were compared to the shelter transpiration results obtained from measurements of sap flow in tree trunks made with thermal dissipation probes and the latent heat fluxes observed by the eddy covariance technique at flux towers in croplands. The modified P-M formula was found to be an effective means to estimate not only the cropland and orchard ET but also the shelter transpiration. The seasonal variation of shelterbelt transpiration was smaller than those of cropland and orchard ET. Estimates of ET made using the P-M formula along with the remote sensing data showed that 9.9%, 3.1%, and 87.0% of the total ET were allotted to shelterbelts, apple orchards, and cropland, respectively.

**Index Terms**—Evapotranspiration (ET), remote sensing, shelterbelt, transpiration, vegetation.

## I. INTRODUCTION

TRANSPIRATION from shelterbelts is an important part of water consumption in the oases in northwest China. Quantitative estimation of the transpiration from plant leaves and the evaporation from soil surfaces in an irrigated area, especially in oases in arid regions, is useful for the management of the limited water resources. Transpiration plays an important role in energy and water exchanges between the land surface and the atmosphere. Evapotranspiration (ET) includes soil evaporation and canopy transpiration, and it plays an important role in energy and water exchange between the land surface and the atmosphere. Approximately 70% of the precipitation that

reaches the Earth's surface returns to the atmosphere through ET action, and in arid areas, the amount can be as high as 90% [2].

With the development of remote sensing technology, estimation models of regional ET have been developed in the past three decades, including statistical models [3], [4], the energy balance residual method [5], the Normalized Difference Vegetation Index (NDVI) and the surface temperature space [6], [7], the 4-D data assimilation method [8], [9], and those from studies that estimated ET by combining remote sensing data with the traditional ET method [10]–[14].

Airborne remote sensing can provide high spatial resolution reflectance data and detailed land cover information, such as the presence of shelterbelts, which is helpful in estimating the water consumption of shelterbelts. In this letter, we used airborne remote sensing data and meteorological data to estimate daily transpiration and ET in the irrigation area in the middle reaches of the Heihe River. The results were compared with thermal dissipation probe (TDP) observations and flux tower observations. In addition, we analyzed the patterns of shelterbelt transpiration and the differences between the shelterbelt and other vegetation types.

## II. DATA AND METHODS

### A. Study Area and Data

The study area is located in the irrigated area in the middle reaches of the Heihe River in northwestern China (Fig. 1), which covers approximately 0.14 million km<sup>2</sup> and is predominantly composed of alpine regions and arid areas. The climate belongs to a typical temperate continental climate, with an annual average temperature of 7.6 °C and an annual rainfall of 113.8 mm. “The Multi-Scale Observation Experiment on Evapotranspiration over heterogeneous land surfaces 2012” in “Heihe Watershed Allied Telemetry Experimental Research” (HiWATER-MUSOEXE) [15], [16] project was conducted from June to September 2012. The observations in the experiment included the climate data, the heat flux from different land covers, and the sap flow rates of the trees in the shelterbelts. Our study area was in the core area of HiWATER-MUSOEXE. There are five heat flux observation sites (EC-6, EC-8, EC-15, EC-16, and EC-17) and three thermal dissipation sap flow probe (TDP) sites in our study area. The EC-6, EC-8, EC-15, and

Manuscript received January 25, 2014; revised May 16, 2014; accepted June 11, 2014. This work was supported by the National Natural Science Foundation of China (91125002). (Corresponding author: Rui Sun.)

C. Qiao and R. Sun are with the State Key Laboratory of Remote Sensing Science, School of Geography, Beijing Normal University, Beijing 100875, China, and also with Beijing Key Laboratory of Environmental Remote Sensing and City Digitalization, Beijing 100875, China (e-mail: qiaochenbnu@gmail.com; sunrui@bnu.edu.cn).

Z. Xu, L. Zhang, L. Hao, and G. Jiang are with the School of Geography, Beijing Normal University, Beijing 100875, China (e-mail: xuzw@bnu.edu.cn; zhangleiai66@126.com; rwatermoon@gmail.com; jianggq@mail.bnu.edu.cn).

L. Liu is with the Institute of Remote Sensing and Digital Earth, Chinese Academy of Sciences, Beijing 100094, China (e-mail: liuliangyun@sina.com). Digital Object Identifier 10.1109/LGRS.2014.2342219

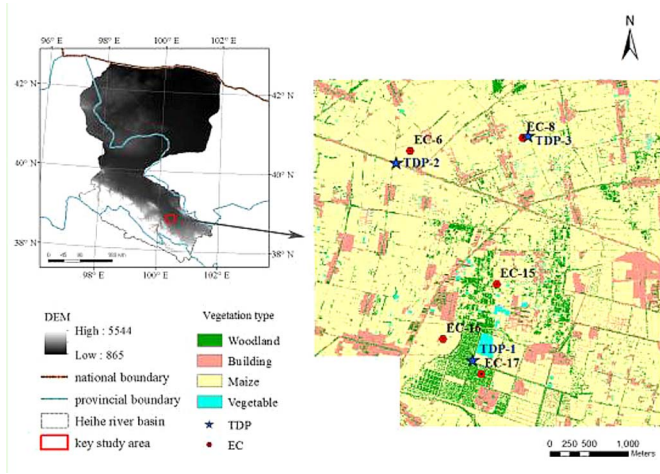


Fig. 1. Location and land cover map of the study area.

EC-16 heat flux sites were in maize fields, and EC-17 was in an apple orchard. The methods of data processing and quality control for the heat flux data are presented in [17].

During the observation periods (from June 14 to September 20), there were 26 rainy days. The total rainfall was 103.1 mm, with 31.1, 47.1, 24.5, and 0.4 mm in June, July, August, and September, respectively. The mean air temperatures at EC-6, EC-8, EC-15, EC-16, and EC-17 were 19.80, 19.72, 19.96, 20.06, and 19.30 °C, respectively.

The airborne remote sensing data were acquired by the Compact Airborne Spectrographic Imager (CASI 1500, ITRES Company, Canada) on June 29, 2012. There are 48 channels on the imager, and the spectral band coverage range is from 382.5 to 1055 nm. The spatial resolution of the imager is 1 m, and the spectral resolution is 7.2 nm. After atmospheric correction with 6s software, the ground and atmospheric synchronous measurement data and the surface reflectance, including albedo products, were produced from the CASI data [18]. The Simple Ratio Vegetation Index (SR) was derived from the red reflectance ( $\rho_r$ ) and near infrared reflectance ( $\rho_{nir}$ ) data ( $SR = \rho_r / \rho_{nir}$ ). The land cover map was also produced from the CASI image [18], with an overall classification accuracy of 91.6%. The land cover in the study area consists of trees, which are mainly *Populus gansuensis* and form shelterbelts on the roadside and the edge of plots, cropland cultivated with maize and vegetables, and apple orchards.

### B. ET Estimation Method

Zhang *et al.* [1] developed a modified Penman–Monteith (P-M) approach to estimate global long-term daily ET with biome-specific canopy conductance. We used this method to estimate the daily evaporation and transpiration in the study area.

In this ET formula, the net radiation  $R_n$  (in watts per square meter) is calculated using

$$R_n = R_{ns} + R_{nl} = (1 - \alpha)R_{s\downarrow} + R_{nl} \quad (1)$$

where  $R_{ns}$  is the net shortwave radiation,  $R_{s\downarrow}$  is the incoming shortwave radiation,  $\alpha$  is the albedo of the surface, and  $R_{nl}$  is the net long-wave radiation. The incoming shortwave radiation

and the net longwave radiation observed at the flux towers and the CASI albedo were used to estimate the net radiation.

The ET was divided into canopy transpiration and soil evaporation. The available energy for ET ( $A$  in watts per square meter) is determined as the difference between  $R_n$  and the soil heat flux ( $G$  in watts per square meter). Because the soil heat flux is approximately zero on the daily scale, we neglected the soil heat flux during the estimation of the daily ET and transpiration in this study.

The  $A$  term is then linearly partitioned into the available energy components for the canopy ( $A_{Canopy}$  in watts per square meter) and the soil surface ( $A_{Soil}$  in watts per square meter) using the fractional vegetation cover ( $f_c$ ), such that

$$A_{Canopy} = A \times f_c \quad (2)$$

$$A_{Soil} = A \times (1 - f_c) \quad (3)$$

The P-M equation is used to calculate the vegetation transpiration as

$$\lambda E_{Canopy} = \frac{\Delta A_{Canopy} + \rho C_p VPD g_a}{\Delta + \gamma(1 + g_a/g_c)} \quad (4)$$

where  $\lambda E_{Canopy}$  (in watts per square meter) is the latent heat flux of the canopy,  $\lambda$  (joules per kilogram) is the latent heat of vaporization,  $\Delta$  (in pascals per kelvin) is the slope of the curve relating the saturated water vapor pressure to the air temperature,  $\rho$  (in kilograms per cubic meter) is the air density,  $C_p$  (in joules per kilogram kelvin) is the specific heat capacity of air, VPD (in pascals) is the vapor pressure deficit,  $g_a$  (in meters per second) is the aerodynamic conductance,  $\gamma$  (in pascals per kelvin) is the psychrometric constant, and  $g_c$  (in meters per second) is the canopy conductance.

Zhang *et al.* [1] estimated canopy conductance using the normalized vegetation index (NDVI). However, the NDVI will saturate at higher vegetation covers, which might underestimate the canopy conductance when the leaf area index (LAI) is higher. Kelliher *et al.* [20] developed an expression for the canopy conductance in terms of several factors, including the maximum stomatal conductance of the leaves at the top of the canopy  $g_{sx}$  (in meters per second), the LAI value, and a hyperbolic response to the absorbed shortwave radiation. Leuning *et al.* [21] modified this expression to include the response of stomatal conductance to humidity deficits. We used this expression to estimate the canopy conductance

$$g_c = \frac{g_{sx}}{K_Q} \ln \left[ \frac{Q_h + Q_{50}}{Q_h \exp(-K_Q LAI) + Q_{50}} \right] \left[ \frac{1}{1 + VPD/D_{50}} \right] \quad (5)$$

where  $g_{sx}$  is the maximum stomatal conductance,  $Q_h$  (in watts per square meter) is the flux density of visible radiation at the top of the canopy (approximately half of incoming solar radiation),  $k_Q$  is the extinction coefficient for shortwave radiation, and  $Q_{50}$  (in watts per square meter) is the visible radiation flux when the stomatal conductance is half its maximum value.  $D_{50}$  (in pascals) is the humidity deficit at which the stomatal conductance is half of its maximum value. The values of  $k_Q$ ,  $Q_{50}$ , and  $D_{50}$  vary with vegetation type and are described in [21].

The LAI value of the irrigation area was estimated using the following equation [22], which was established for the same region:

$$\text{LAI} = 4.46471 - 11.62975 \exp\left(\frac{-\text{SR}}{0.91739}\right) \quad (6)$$

The soil evaporation is calculated as

$$\lambda E_{\text{Soil}} = \text{RH} \left(\frac{\text{VPD}}{k}\right) \frac{\Delta A_{\text{Soil}} + \rho C_p \text{VPD} g_a}{\Delta + \gamma \times g_a / g_{\text{totc}}} \quad (7)$$

where  $\lambda E_{\text{Soil}}$  (in watts per square meter) is the latent heat flux of soil, RH is the relative humidity of air,  $k$  (in pascals) is a parameter to fit the complementary relationship that reflects the relative sensitivity to VPD, and  $g_{\text{totc}}$  (in meters per second) is the corrected value of the total aerodynamic conductance. The formula is described in detail in [1].

### C. Sap Flow Measurement

We utilized the TDP [23] to measure the sap flow through the tree trunk. We selected three sites for the measurement and selected three poplar trees in each site.

Three TDPs were inserted into each trunk at a height of 1.3 m, and each TDP had two probes. The temperature difference between the two probes was influenced by the sap flux density in the vicinity of the heated probe. The mean sap flux density  $V$  (in centimeters per hour) was calculated from the following relation [23]:

$$V = 3600 \times 0.0119 \times \left(\frac{\Delta T}{\Delta T_m} - 1\right)^{1.231} \quad (8)$$

where  $\Delta T_m$  and  $\Delta T$  are the temperature differences between the two probes for the no-flow and positive xylem flow ( $V > 0$ ) conditions, respectively.  $\Delta T_m$  was determined by the maximum temperature difference in a day, which generally occurred at predawn.

The total sap flow  $F$  (in cubic centimeters per hour) is calculated in the following way:

$$F = A \times V \quad (9)$$

in which

$$A = \pi \times \left[ \left(\frac{D}{2} - \Delta D\right)^2 - \left(\frac{D_1}{2}\right)^2 \right] \quad (10)$$

where  $A$  is the cross-sectional area of the sapwood at the heating probe (in square centimeters),  $D$  is the diameter of the tree under evaluation,  $D_1$  is the pith diameter, and  $\Delta D$  is the bark thickness; the units are in centimeters. The sapwood area was measured with an increment borer; the maximum error was 10%.

We measured the shelterbelt area of each experimental site and the density of the trees and then calculated the daily shelterbelt transpiration per unit area ( $Q$  in millimeters per day) according to the total sap flow and the shelterbelt area. The equation used is as follows:

$$Q = \frac{F_d}{S} \quad (11)$$

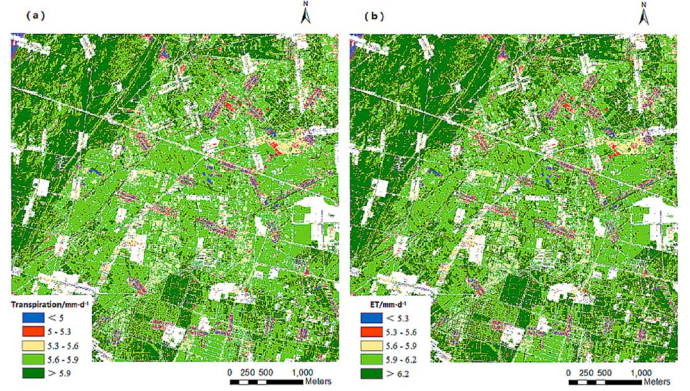


Fig. 2. Spatial distribution of (a) daily canopy transpiration and (b) daily ET on June 29, 2012.

where  $F_d$  is the total daily sap flow and  $S$  is the corresponding area of the shelterbelt.

## III. COMPARISONS BETWEEN ESTIMATE RESULTS AND OBSERVATIONS

Assuming no changes in the SR or surface albedo during the ten-day period, the airborne remotely sensed CASI data acquired on June 29, 2012, and the daily observed meteorological data were used to estimate the daily transpiration and ET from June 25 to July 4. The ET at the build-up area was not calculated. Fig. 2 shows the spatial pattern of the transpiration and ET on June 29, 2012. It can be seen from the figure that the daily transpiration ranged from 0.1 to 7.0 mm and that the average transpiration of the study area was 5.7 mm, with most of the data concentrated in the range from 4.7 to 6.5 mm. Accordingly, the daily ET ranged from 0.5 to 7.5 mm, and the average ET was 6.1 mm, with most of the data concentrated in the range from 5.0 to 6.6 mm. The ET from the shelterbelt was higher than that from the other vegetation types.

### A. Comparison of P-M and TDP Transpiration

We determined the statistics of the average shelterbelt transpiration at three TDP sites from the remote sensing estimation results and then compared the results with the corresponding TDP measurements from June 25 to July 4 (Fig. 3).

Fig. 3 demonstrates that the remote sensing method is effective in estimating the transpiration of the shelterbelt. The determination coefficient between the P-M results and the TDP observations is 0.438, and the root-mean-square error (rmse) is  $1.03 \text{ mm} \cdot \text{day}^{-1}$ . The transpiration value obtained using the P-M formula was consistent with the TDP observations. The average transpiration from the TDP observations was  $4.0 \text{ mm} \cdot \text{day}^{-1}$ , and the result from the P-M formula was  $4.1 \text{ mm} \cdot \text{day}^{-1}$ . However, in the observation period, underestimation of the transpiration on the rainy days (June 26 and June 27, with rainfall values of 2.6 and 15.6 mm, respectively) can be clearly observed from the figure, with the observations revealing transpiration of  $2.2\text{--}4.0 \text{ mm} \cdot \text{day}^{-1}$  and the estimation providing a transpiration value of approximately  $2.1 \text{ mm} \cdot \text{day}^{-1}$ . The results also indicate that both the model

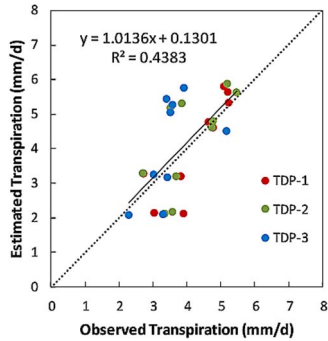


Fig. 3. Shelterbelt transpiration by P-M formula compared with TDP observations (in millimeters per day).

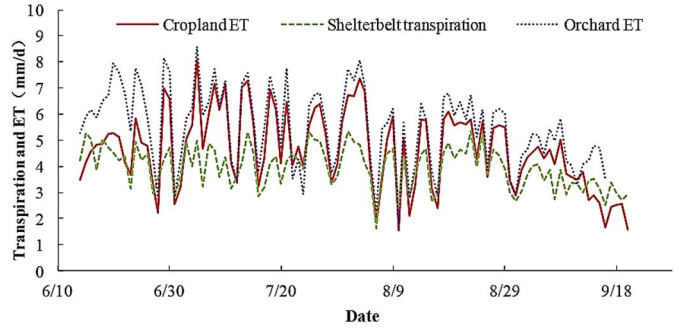


Fig. 5. Dynamic change of transpiration and ET for the shelterbelt, cropland, and orchard (June 14 to September 20, 2012).

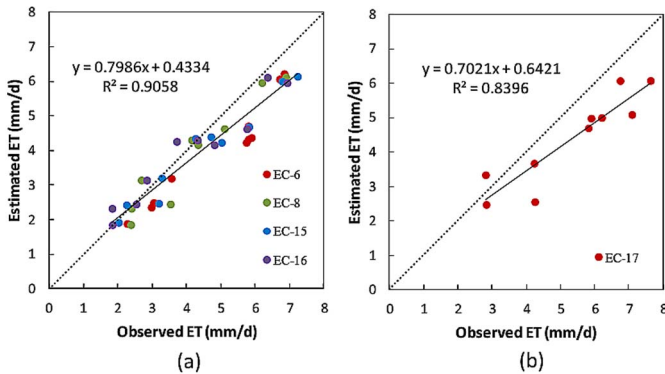


Fig. 4. Comparison of modeled and observed daily ET (in millimeters per day). The two figures represent two vegetation types, including (a) cropland and (b) orchard.

shelterbelt transpiration and the observations at the TDP-1 and TDP-2 sites were higher than those at the TDP-3 site, which is related to the soil moisture and the size of the trees. In fact, the TDP-1 site is close to the apple orchard, and the TDP-2 site is close to the main canal, resulting in sufficient soil moisture, large crown, and higher transpiration, whereas the TDP-3 site has a relatively low crown and lower transpiration. Sufficient soil moisture caused the relatively low surface albedo at the TDP-1 and TDP-2 sites, which resulted in more available energy for transpiration. The albedo value retrieved from the CASI image shows that the surface albedo values at the TDP-1, TDP-2, and TDP-3 sites were 0.150, 0.140, and 0.156, respectively.

**B. Comparison of P-M ET and ET Observed at Flux Towers**

The remotely sensed ET values were compared with the latent heat flux data observed from five flux towers near the TDP sites (Fig. 4). Among these flux towers, the vegetation at sites EC-6, EC-8, EC-15, and EC-16 is maize, whereas the land cover type at site EC-17 is an apple orchard.

The comparison indicated that the ET results derived by remote sensing were highly correlated with the observations, with determination coefficients of 0.905 and 0.839 for cropland and orchard, respectively. The underestimation of ET can also be observed from the figure. The average ET values from cropland and orchard from the flux tower observations were 4.41 and 5.35 mm · day<sup>-1</sup>, respectively, and the ET values

using the P-M formula for cropland and orchard were 3.95 and 4.40 mm · day<sup>-1</sup>, respectively. The calculated ET from the cropland was closer to the observations, with an rmse of 0.71 mm · day<sup>-1</sup> and a relatively large error on sunny days, while the rmse of the orchard was 1.18 mm · day<sup>-1</sup>.

For these five eddy covariance flux tower sites and three TDP sites, the transpiration and ET determined by the P-M formula exhibited comparable results, with the best results for the cropland ET, slightly poorer results for the shelterbelt transpiration, and largest error in ET for the orchard. The results demonstrate that, although the modified P-M formula can be used to estimate the daily transpiration and the ET with airborne remote sensing data, it results in underestimations compared with the flux tower observations. In the modified P-M formula, the canopy conductance  $g_c$  functions play a vital role. In addition, the canopy conductance parameters in the model can influence the estimation results. The optimization of these parameters and of the  $g_c$  functions might improve model performance.

**IV. SEASONAL VARIATION OF ET**

Using the latent heat flux data observed for the cropland and orchard, and the shelterbelt transpiration derived from the three TDP observation points from June 14 to September 20, the dynamic change in transpiration and ET for different vegetation types was analyzed (Fig. 5).

The patterns of shelterbelt transpiration and ET from the cropland and orchard were similar from June to September. The transpiration and ET in July were relatively large for all vegetation types. The variations in shelterbelt transpiration were small, whereas the ET variations for the cropland and orchard were larger. The ET from the cropland and orchard was generally higher than the shelterbelt transpiration during the observation period. However, by early September, the cropland ET began to rapidly decrease, and it became lower than the shelterbelt transpiration by the middle of September due to the harvesting of the maize. During this period, the ET of the orchard also declined due to the soil evaporation between the trees in the orchard, although it remained higher than the shelterbelt transpiration.

We used the modeled daily ET from June 25 to July 4 and the land cover classification map to calculate the total ET of the different vegetation types and analyze the proportion

TABLE I  
ET OF DIFFERENT VEGETATION TYPES AND THEIR  
PROPORTION OF THE TOTAL ET

Vegetation type	Area (km <sup>2</sup> )	ET (m <sup>3</sup> d <sup>-1</sup> )	ET proportion of total ET (%)
Shelterbelt	1.39	6527.5	9.9
Orchard	0.53	2020.8	3.1
Cropland	14.59	57463.0	87.0

of ET for each vegetation type in the study area (Table I). The results indicated that the shelterbelt ET accounted for approximately 9.9% of the total ET, the orchard ET accounted for approximately 3.1%, and the cropland ET accounted for approximately 87.0%.

## V. CONCLUSION

Airborne remote sensing data and a modified P-M model [1] were used to estimate the ET from an irrigation area in the middle reaches of the Heihe River basin. A comparison between the modeled results and the *in situ* observations indicated that the ET and the shelterbelt transpiration estimations generally agreed with the flux tower and the TDP observations, with the best results for the cropland ET, which demonstrates that, although the model was originally developed to estimate global ET, it can also estimate the daily transpiration and the ET with fine spatial resolution remote sensing data.

The dynamic changes in the shelterbelt transpiration and the ET of the cropland and the orchard were similar from June to September. The transpiration and the ET in July were relatively higher for all vegetation types. The seasonal variation in the shelterbelt transpiration was smaller than the ET changes in the cropland and the orchard.

From June 25 to July 4, the shelterbelt ET accounted for approximately 9.9% of the total ET, the orchard ET accounted for approximately 3.1%, and the cropland ET accounted for approximately 87.0%.

## ACKNOWLEDGMENT

The authors would like to thank all of the scientists, engineers, and students who participated in the HiWATER field campaigns.

## REFERENCES

- [1] K. Zhang, J. S. Kimball, R. R. Nemani, and S. W. Running, "A continuous satellite-derived global record of land surface evapotranspiration from 1983 to 2006," *Water Resour. Res.*, vol. 46, no. 9, pp. W09522-1–W09522-21, Sep. 2010.
- [2] N. J. Rosenberg, B. L. Blad, and S. B. Verma, *Microclimate: The Biological Environment*, 2nd ed. New York, NY, USA: Wiley, 1983.
- [3] R. D. Jackson, R. J. Reginato, and S. B. Idso, "Wheat canopy temperature: A practical tool for evaluating water requirements," *Water Resour. Res.*, vol. 13, no. 3, pp. 651–656, Jun. 1977.
- [4] B. Seguin and B. Itier, "Using midday surface temperature to estimate daily evaporation from satellite thermal IR data," *Int. J. Remote Sens.*, vol. 4, no. 2, pp. 371–383, Feb. 1983.
- [5] W. G. M. Bastiaanssen, M. Menenti, R. A. Feddes, and A. A. M. Holtslag, "A remote sensing Surface Energy Balance Algorithm for Land (SEBAL): Part 1. Formulation," *J. Hydrol.*, vol. 212/213, pp. 198–212, Dec. 1998.
- [6] T.N. Carlson and M. J. Buffum, "On estimating total daily evapotranspiration from remote surface temperature measurements," *Remote Sens. Environ.*, vol. 29, no. 2, pp. 197–207, Aug. 1989.
- [7] L. Jiang and S. Islam, "Estimation of surface evaporation map over southern Great Plains using remote sensing data," *Water Resour. Res.*, vol. 37, no. 2, pp. 329–340, Feb. 2001.
- [8] Y. Dai *et al.*, "The common land model," *Bull. Amer. Meteorol. Soc.*, vol. 84, no. 4, pp. 1013–1023, Aug. 2003.
- [9] J. M. Schuurmans, P. A. Troch, A. A. Veldhuizen, W. G. M. Bastiaanssen, and M. F. P. Bierkens, "Assimilation of remotely sensed latent heat flux in a distributed hydrological model," *Adv. Water Resour.*, vol. 26, no. 2, pp. 151–159, Feb. 2003.
- [10] J. L. Monteith, "Evaporation and environment," in *Proc. Symp. Soc. Exp. Biol.*, 1965, vol. 19, pp. 205–234.
- [11] C. H. B. Priestley and R. J. Taylor, "On the assessment of surface heat flux and evaporation using large-scale parameters," *Mon. Weather Rev.*, vol. 100, no. 2, pp. 81–92, Feb. 1972.
- [12] W. Brutsaert and H. Stricker, "An advection-aridity approach to estimate actual regional evapotranspiration," *Water Resour. Res.*, vol. 15, no. 2, pp. 443–450, Apr. 1979.
- [13] F. I. Morton, "Operational estimates of areal evapotranspiration and their significance to the science and practice of hydrology," *J. Hydrol.*, vol. 66, no. 1–4, pp. 1–76, Oct. 1983.
- [14] R. J. Granger, "A complementary relationship approach for evaporation from nonsaturated surfaces," *J. Hydrol.*, vol. 111, no. 1–4, pp. 31–38, Nov. 1989.
- [15] Z. W. Xu *et al.*, "Intercomparison of surface energy flux measurement systems used during the HiWATER-MUSOEXE," *J. Geophys. Res.*, vol. 118, no. 23, pp. 13 140–13 157, Dec. 2013.
- [16] X. Li *et al.*, "Heihe Watershed Allied Telemetry Experimental Research (HiWATER): Scientific objectives and experimental design," *Bull. Amer. Meteorol. Soc.*, vol. 94, no. 8, pp. 1145–1160, Aug. 2013.
- [17] S. M. Liu *et al.*, "A comparison of eddy-covariance and large aperture scintillometer measurements with respect to the energy balance closure problem," *Hydrol. Earth Syst. Sci.*, vol. 15, no. 4, pp. 1291–1306, Apr. 2011.
- [18] Q. Xiao and J. G. Wen, "HiWATER: Visible and near-infrared hyperspectral radiometer," *Inst. Remote Sens. Digit. Earth, Chinese Acad. Sci.*, Beijing, China, Jun. 29, 2012.
- [19] Z. H. Wang and L. Y. Liu, "Monitoring on land cover pattern and crops structure of oasis irrigation area of middle reaches in Heihe River basin using remote sensing data," *Adv. Earth Sci.*, vol. 28, no. 8, pp. 948–956, Aug. 2013.
- [20] F. M. Kelliher, R. Leuning, M. R. Raupach, and E. D. Schulze, "Maximum conductances for evaporation from global vegetation types," *Agric. Forest Meteorol.*, vol. 73, no. 1/2, pp. 1–16, Feb. 1995.
- [21] R. Leuning, Y. Q. Zhang, A. Rajaud, H. Cleugh, and K. Tu, "A simple surface conductance model to estimate regional evaporation using MODIS leaf area index and the Penman–Monteith equation," *Water Resour. Res.*, vol. 44, no. 10, pp. W10419-1–W10419-17, Oct. 2008.
- [22] Q. Z. Xu, W. G. Zhang, S. C. Liu, D. Z. Zhao, and J. J. Jiang, "Retrieval of leaf area index for the Heihe River watershed by using remote sensing data," *Arid Zone Res.*, vol. 20, no. 4, pp. 281–285, Dec. 2003 Chinese.
- [23] A. Grainer, "Evaluation of transpiration in a Douglas fir stand by means of sap flow measurement," *Tree Physiol.*, vol. 3, no. 4, pp. 309–320, Apr. 1987.